

## SUPPLEMENTARY FIGURE LEGENDS

Supplementary Fig. S1. Vaccination does not change N-803 mediated trafficking of CD8 T cells. A, Frozen PBMC that were isolated from whole blood samples collected from the indicated timepoints pre- and post- N-803 treatment were stained for flow cytometric analysis as indicated in Table 2. Complete white blood cell counts (CBC) were used to quantify the absolute number of CD3<sup>+</sup> cells that were CD8<sup>+</sup>tetramer<sup>-</sup> (top), Gag<sub>181-189</sub>CM9 tetramer<sup>+</sup>(middle), and Tat<sub>28-35</sub>SL8 tetramer<sup>+</sup> (bottom) cells per  $\mu$ L of blood. The results were then normalized to the average value for the absolute counts for each cell population from pre-N-803 controls and are displayed as the fold change in absolute cell counts/ $\mu$ L blood. Repeated measures ANOVA non-parametric tests were performed, with Dunnett's multiple comparisons for individuals across multiple timepoints. For individuals for which samples from timepoints were missing, mixed-effects ANOVA tests were performed using Geisser-Greenhouse correction. \*,  $p \leq 0.05$ ; \*\*,  $p \leq 0.005$ ; \*\*\*,  $p \leq 0.0005$ ; \*\*\*\*,  $p \leq 0.0001$ . B, Lymph nodes were collected from the indicated timepoints pre- and post- N-803 treatment. Cells were stained from frozen samples as indicated in (A) for flow cytometric analysis. The frequencies of CD3<sup>+</sup> T cells that were CD8<sup>+</sup>SIV tetramer<sup>-</sup> (top panel), CD8<sup>+</sup>Gag<sub>181-189</sub>CM9 tetramer<sup>+</sup>(middle), or CD8<sup>+</sup>Tat<sub>28-35</sub>SL8 tetramer<sup>+</sup> (bottom) were determined, then the data were normalized to the average of the pre N-803 frequencies. Statistical analysis was performed as described in (A). p=ns; not significant.

Supplementary Fig. S2. Representative gating schematic for Tetramer<sup>+</sup> cells and memory markers in *Mamu-A\*001*<sup>+</sup> and *Mamu-B\*008*<sup>+</sup> macaques. A, Frozen PBMC from all *Mamu-A\*001*<sup>+</sup> macaques in this study were stained with the antibodies indicated in Table 2 of the methods. Flow

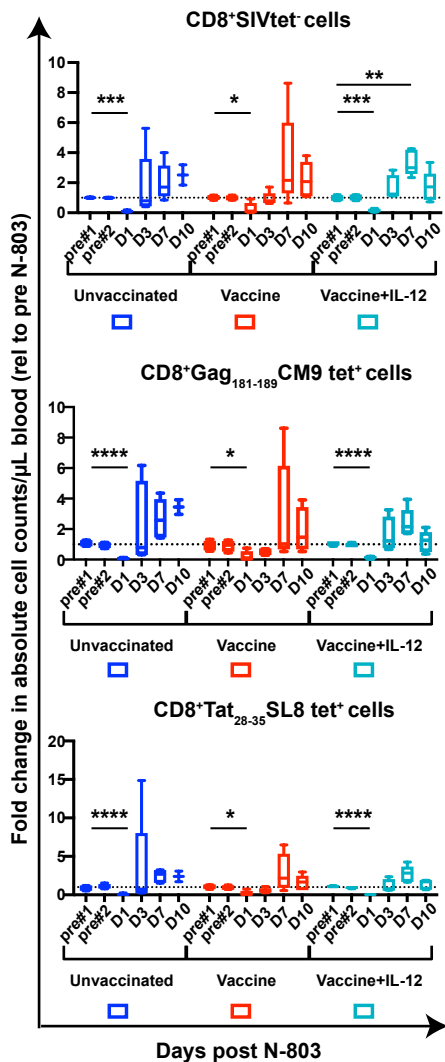
cytometry was performed as described in the methods. Shown is a representative gating schematic for CD8+Gag<sub>181-189</sub>CM9 tetramer+, CD8+Tat<sub>28-35</sub>SL8 tetramer+, and CD8+SIV tetramer- cells, and memory sub-populations for each respective tetramer-positive or -negative parent population. B, Representative gating schematic for Nef<sub>137-146</sub>RL10 tetramer+ cells in B\*008+ macaques. Cells were stained identically to the samples in (A) except Nef<sub>137-146</sub>RL10 tetramer was used instead of Gag<sub>181-189</sub>CM9 tetramer, and no Tat<sub>28-35</sub>SL8 tetramer was used. Shown is a representative sample indicating Nef<sub>137-146</sub>RL10 tetramer+ cells and the memory subpopulations of those cells. C, Gating schematic used to define Effector memory, Central memory, and Transitional memory cells. Memory subpopulations that were shown in (A) and (B) were further differentiated into effector memory (CD28-CD95+CCR7-), transitional memory (CD28+CD95+CCR7-) or central memory (CD28+CD95+CCR7+) based on CCR7 expression. Central memory and transitional memory cell phenotypes were validated by examining CCR7 expression based on the CD28+CD95+ parent gate.

Supplementary Fig. S3. Representative gating schematic for ki-67 and Granzyme B expression on SIV specific cells of SIV controllers and non-controllers. Frozen PBMC from SIV controllers (gold; top panels) or SIV non-controllers (purple, bottom panels) were stained with the antibodies indicated in Table 2 of the methods, and flow cytometry was performed. The frequency of ki-67+ and GranzymeB+ cells were determined for all memory subpopulations of CD8+SIV tetramer-, Gag<sub>181-189</sub>CM9 tetramer+, Nef<sub>137-146</sub>RL10 tetramer+, and Tat<sub>28-35</sub>SL8 tetramer+ cells. Shown is representative ki-67 and Granzyme B staining for the effector memory (EM) cells of Gag<sub>181-189</sub>CM9 tetramer+ cells of an SIV controller (gold) and an SIV non-controller (purple) from pre N-803 and Day 3 post N-803 timepoints.

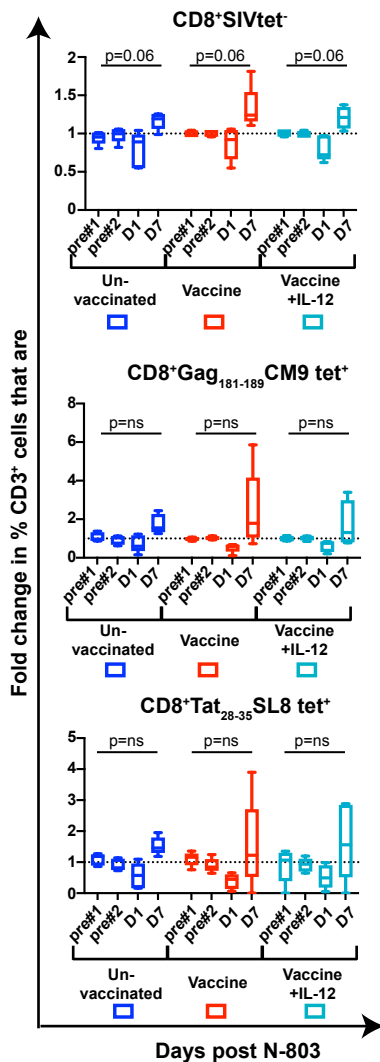
Supplementary Fig. S4. A, Representative gating schematic for intracellular cytokine staining (ICS) assay. Frozen PBMC from SIV non-controllers (purple) or SIV controllers (gold) were incubated overnight with media alone (no stim), or stimulated with peptides as indicated in the methods. For this representative figure, 0.5 $\mu$ g/mL of Gag<sub>181-189</sub>CM9 peptide was used. The following day, the cells were stained with the antibodies indicated in Table 4 of the methods, and flow cytometry was performed. Shown is a gating schematic for CD8<sup>+</sup> T cells, and representative CD107a<sup>+</sup>, TNF $\alpha$ <sup>+</sup>, IFN $\gamma$ <sup>+</sup> subpopulations with each respective stimulus for an SIV controller (gold) and an SIV non-controller (purple). B, Frequencies of CD107a<sup>+</sup>, IFN $\gamma$ <sup>+</sup>, or TNF $\alpha$ <sup>+</sup> from intracellular cytokine staining assays from Fig. 8 prior to background subtraction. Intracellular cytokine staining assays were performed as indicated in Fig. 8 and cells were stained as indicated in Table 4. Shown are the frequencies of CD8 T cells producing CD107a (left), IFN $\gamma$  (middle), or TNF $\alpha$  (right) prior to background subtraction. NS; no stim, pep; 0.5 $\mu$ g/mL of Gag<sub>181-189</sub>CM9 or Nef<sub>137-146</sub>RL10 peptides, pool; 0.5 $\mu$ g/mL of SIVmac239 Gag peptide pool.

# Supplementary Fig. S1

## A PBMC analysis

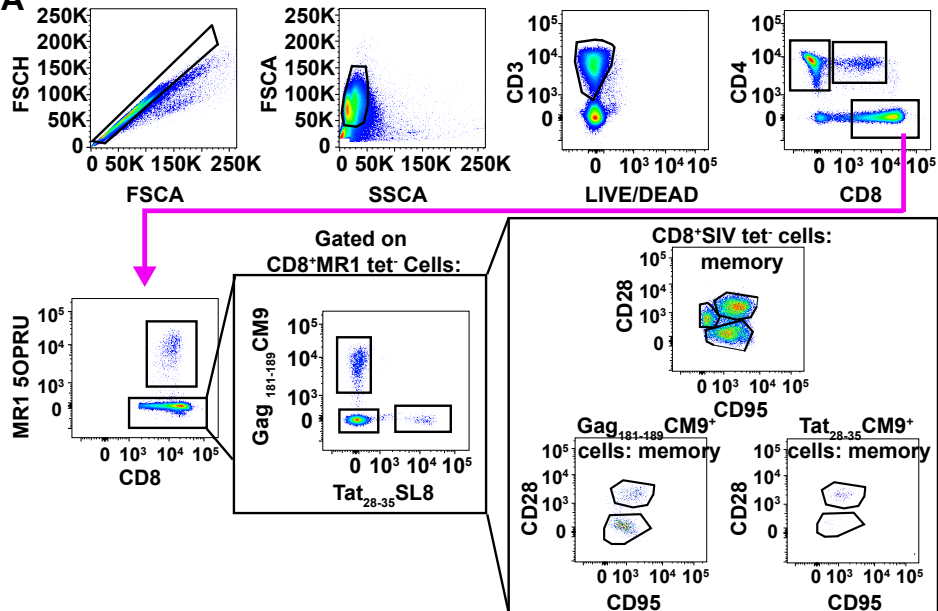


## B Lymph node analysis

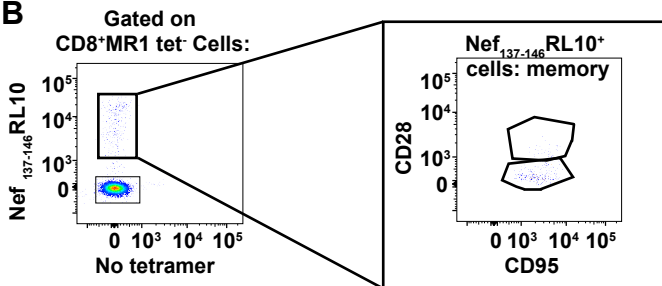


# Supplementary Fig. S2

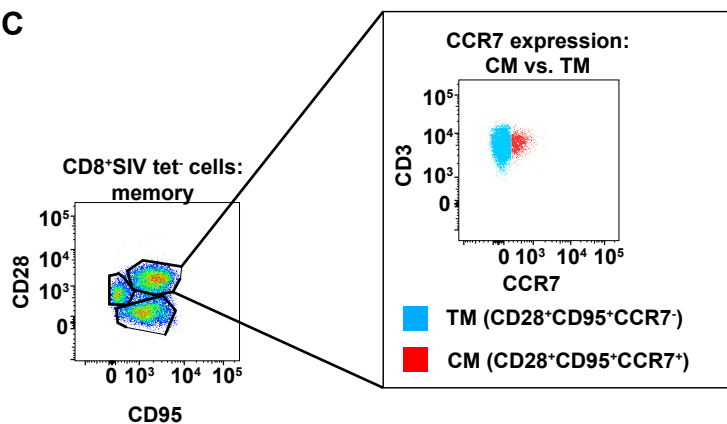
## A



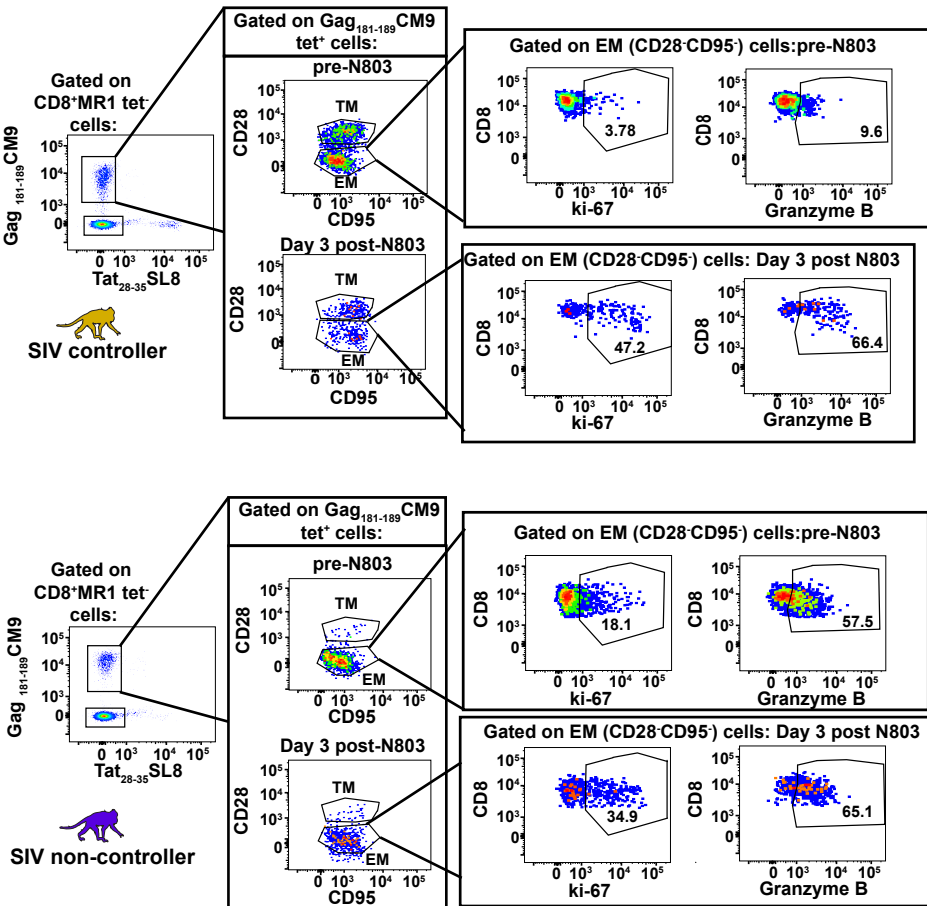
## B



## C

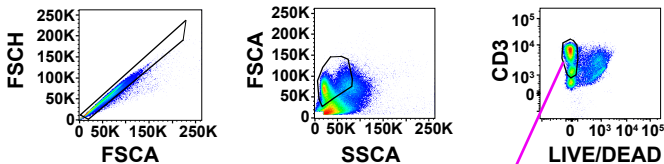


# Supplementary Fig. S3



# Supplementary Fig. S4

## A

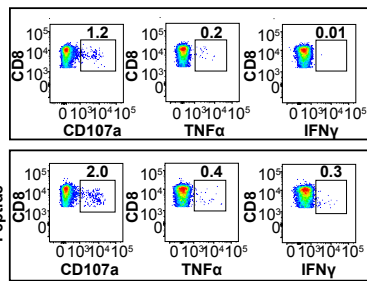
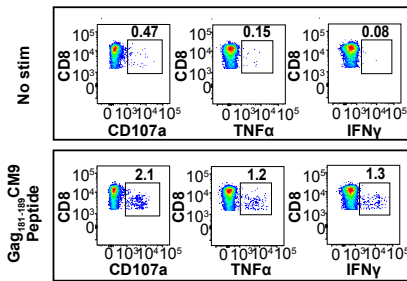


**SIV controller**

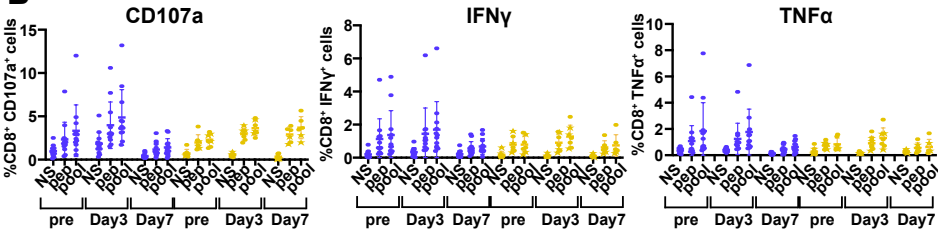
**SIV non-controller**

**Stimulus:**

**Stimulus:**



## B



**Non-controllers**      **Controllers**